

Nodeless superconductivity in $\text{Ir}_{1-x}\text{Pt}_x\text{Te}_2$ with strong spin-orbital coupling

S. Y. Zhou,¹ X. L. Li,¹ B. Y. Pan,¹ X. Qiu,¹ J. Pan,¹ X. C. Hong,¹ Z. Zhang,¹ A. F. Fang,² N. L. Wang,² S. Y. Li^{1,*}

¹*State Key Laboratory of Surface Physics, Department of Physics,
and Laboratory of Advanced Materials, Fudan University, Shanghai 200433, P. R. China*

²*Beijing National Laboratory for Condensed Matter Physics, Institute of Physics,
Chinese Academy of Sciences, Beijing 100190, P. R. China*

(Dated: June 22, 2018)

The thermal conductivity κ of superconductor $\text{Ir}_{1-x}\text{Pt}_x\text{Te}_2$ ($x = 0.05$) single crystal with strong spin-orbital coupling was measured down to 50 mK. The residual linear term κ_0/T is negligible in zero magnetic field. In low magnetic field, κ_0/T shows a slow field dependence. These results demonstrate that the superconducting gap of $\text{Ir}_{1-x}\text{Pt}_x\text{Te}_2$ is nodeless, and the pairing symmetry is likely conventional s -wave, despite the existence of strong spin-orbital coupling and a quantum critical point.

PACS numbers: 74.25.fc, 74.40.Kb, 74.25.Op

I. INTRODUCTION

The effect of strong spin-orbital coupling (SOC) on superconductivity has recently attracted much attention. One example is the topological superconductor, such as candidate $\text{Cu}_x\text{Bi}_2\text{Se}_3$ in which Cu atoms are intercalated into topological insulator Bi_2Se_3 with strong SOC.¹ Novel superconducting state was claimed in $\text{Cu}_x\text{Bi}_2\text{Se}_3$ by the point-contact spectra and superfluid density measurements.^{2,3} Another example is the noncentrosymmetric superconductor, such as $\text{Li}_2\text{Pt}_3\text{B}$ in which the spatial inversion symmetry is broken.⁴ The strong SOC in $\text{Li}_2\text{Pt}_3\text{B}$ gives large spin-triplet pairing component and produces line nodes in the superconducting gap.^{5,6}

More recently, superconductivity was discovered in the layered compound IrTe_2 by Pd intercalation (Pd_xIrTe_2),⁷ Pd substitution ($\text{Ir}_{1-x}\text{Pd}_x\text{Te}_2$),⁷ Pt substitution ($\text{Ir}_{1-x}\text{Pt}_x\text{Te}_2$),⁸ or Cu intercalation (Cu_xIrTe_2).⁹ Since the SOC is proportional to Z^4 , where Z is the atomic number, the superconductivity in doped IrTe_2 must associated with strong SOC due to the large Z .

Furthermore, the parent compound IrTe_2 exhibits an intriguing structural phase transition from a high-temperature trigonal to a low-temperature monoclinic phase near 270 K.⁷ Initially it was related to a charge-density-wave (CDW) induced by Ir $5d$ t_{2g} orbitals,^{7,10} however, later no CDW gap was detected from the optical spectroscopy¹¹ and angle-resolved photoemission spectroscopy (ARPES)¹² measurements. At this moment, the origin of the transition is still under hot debate, with proposals such as crystal field effect from Te $5p$ orbital splitting,¹¹ the depolymerization-polymerization of anionic Te bonds,¹³ and Ir $5d$ orbital order.¹⁴ With increasing the doping level x , the structure transition is gradually suppressed and superconductivity emerges, showing a dome-like phase diagram with the maximum T_c of 3 K near $x \approx 0.04$.^{7,8} Such a phase diagram of doped IrTe_2 is reminiscent of high- T_c cuprates and some heavy fermion superconductors, in which superconductivity appears close to a magnetic quantum critical point (QCP).

This means that there likely exists a QCP under the superconducting dome of doped IrTe_2 , and the superconductivity may be unconventional.¹⁵ Therefore it is of great interest to investigate whether there is novel superconducting state in doped IrTe_2 .

The ultra-low-temperature thermal conductivity measurement is a bulk tool to study the gap structure of superconductors.¹⁶ The existence of a finite residual linear term κ_0/T in zero field is usually considered as the signature of nodal superconducting gap. Further information of nodal gap, gap anisotropy, or multiple gaps may be obtained from the field dependence of κ_0/T .¹⁶ Previously, single-gap s -wave superconductivity near the QCP of CDW has been clearly shown in Cu_xTiSe_2 by thermal conductivity measurements.¹⁷

In this paper, we probe the superconducting gap structure of $\text{Ir}_{1-x}\text{Pt}_x\text{Te}_2$ ($x = 0.05$) single crystal by measuring the thermal conductivity κ down to 50 mK. The residual linear term κ_0/T is negligible in zero magnetic field. The field dependence of κ_0/T is slow at low field, unlike that of a nodal superconductor. Both results suggest nodeless superconducting gap in $\text{Ir}_{1-x}\text{Pt}_x\text{Te}_2$.

II. EXPERIMENTAL

Single crystals of $\text{Ir}_{1-x}\text{Pt}_x\text{Te}_2$ were grown via self-flux method.¹¹ The dc magnetic susceptibility was measured by using a SQUID (MPMS, Quantum Design). The heat capacity measurement was performed in a physical property measurement system (PPMS, Quantum Design) via the relaxation method. The $\text{Ir}_{0.95}\text{Pt}_{0.05}\text{Te}_2$ single crystal was cut to a rectangular shape of dimensions 2.0×0.55 mm² in the ab plane and 20 μm thickness along the c axis. Four silver wires were attached to the sample surface with silver paint, which were used for both in-plane resistivity and thermal conductivity measurements. The contacts are metallic with typical resistance 15 m Ω at 2 K. In-plane thermal conductivity was measured in a dilution refrigerator, using a standard four-wire steady-state method with two RuO_2 chip thermometers, calibrated *in*

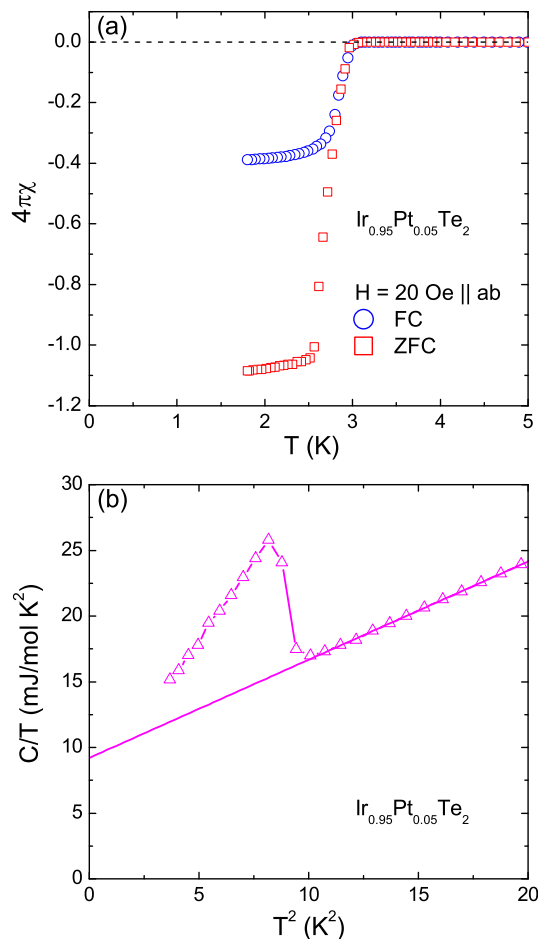


FIG. 1: (Color online). (a) Low-temperature magnetic susceptibility of $\text{Ir}_{0.95}\text{Pt}_{0.05}\text{Te}_2$ single crystal. The measurements were performed in an applied field of $H = 20$ Oe parallel to the ab plane with zero-field-cooled (ZFC) and field-cooled (FC) processes. (b) Specific heat C/T as a function of T^2 for $\text{Ir}_{0.95}\text{Pt}_{0.05}\text{Te}_2$ single crystals. The C/T versus T^2 shows a linear dependence above T_c , giving the electronic specific-heat coefficient $\gamma = 9.20$ mJ/mol K^2 .

situ against a reference RuO_2 thermometer. Magnetic fields were applied along the c axis and perpendicular to the heat current. To ensure a homogeneous field distribution in the sample, all fields for resistivity and thermal conductivity measurements were applied at temperature above T_c .

III. RESULTS AND DISCUSSION

Figure 1(a) presents the dc magnetic susceptibility of $\text{Ir}_{0.95}\text{Pt}_{0.05}\text{Te}_2$ single crystal. It was measured in magnetic field $H = 20$ Oe parallel to the ab plane, with zero-field-cooled (ZFC) and field-cooled (FC) processes. Sharp superconducting transition with $T_c \approx 3.0$ K and about 100% shielding volume fraction were observed for the ZFC process, suggesting the homogeneous bulk su-

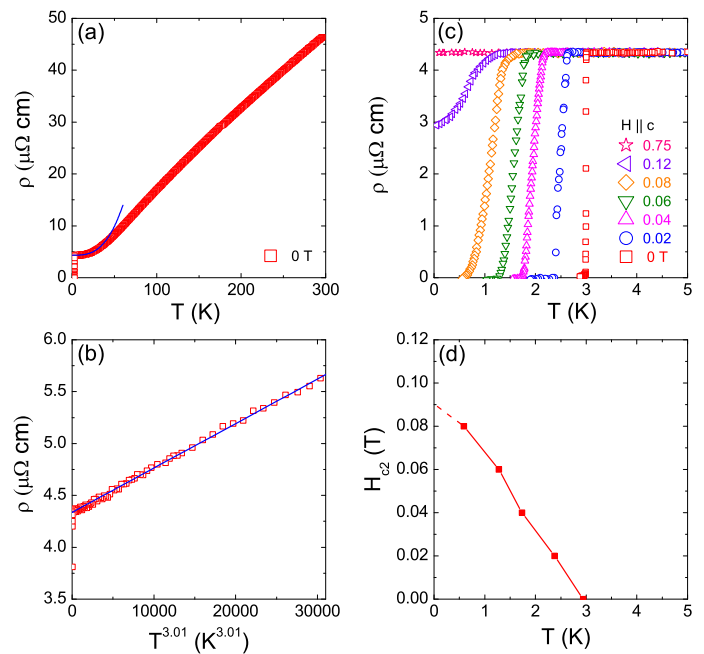


FIG. 2: (Color online). (a) Temperature dependence of the resistivity ρ for $\text{Ir}_{0.95}\text{Pt}_{0.05}\text{Te}_2$ single crystal. The data between 3.5 and 31 K can be fitted to $\rho(T) = \rho_0 + AT^n$, as shown by the solid line, with $\rho_0 = 4.34 \pm 0.002$ $\mu\Omega\text{cm}$ and $n = 3.01 \pm 0.03$. (b) The resistivity ρ as a function of $T^{3.01}$ below 31 K. The solid line is the fitting curve in (a). (c) Low-temperature resistivity of $\text{Ir}_{0.95}\text{Pt}_{0.05}\text{Te}_2$ single crystal in magnetic fields up to 0.75 T. (d) Temperature dependence of the upper critical field H_{c2} , defined at the point ρ dropping to zero on the curves in (c). The dashed line is a guide to the eye, which points to $H_{c2}(0) \approx 0.09$ T.

perconductivity in our sample.

Heat capacity was measured on three pieces of $\text{Ir}_{0.95}\text{Pt}_{0.05}\text{Te}_2$ single crystals, with a total mass of 8.8 mg. It is plotted in Fig. 1(b), as C/T versus T^2 . Above T_c , the data can be well fitted by $C/T = \gamma + \beta T^2$, giving the electronic specific-heat coefficient $\gamma = 9.20$ mJ/mol K^2 . The significant jump was observed at $T_c \approx 3.0$ K, which also indicates the high quality of our single crystals.

Figure 2(a) shows the resistivity of $\text{Ir}_{0.95}\text{Pt}_{0.05}\text{Te}_2$ single crystal in zero field. No resistivity anomaly is observed above T_c , suggesting that no structural transition occurs in this sample near optimal doping. The data between 3.5 and 31 K can be fitted to $\rho(T) = \rho_0 + AT^n$, with $\rho_0 = 4.34 \pm 0.002$ $\mu\Omega\text{cm}$ and $n = 3.01 \pm 0.03$. To see more clearly, Fig. 2(b) plots ρ versus $T^{3.01}$ and the solid line represents the fitting curve data in Fig. 2(a). Such a temperature dependence of $\rho(T) \sim T^n$ with $n \approx 2.8$ has been observed in $\text{Ir}_{1-x}\text{Pt}_x\text{Te}_2$ polycrystal and attributed to phonon-assisted interband scattering,⁸ as in TiSe_2 .¹⁸

Previously, the upper critical field $H_{c2}(0) \approx 0.17$ T has been determined for $\text{Ir}_{0.96}\text{Pt}_{0.04}\text{Te}_2$ polycrystal by resistivity measurements.⁸ In order to obtain the $H_{c2}(0)$ of our $\text{Ir}_{0.95}\text{Pt}_{0.05}\text{Te}_2$ single crystal, we also measure its

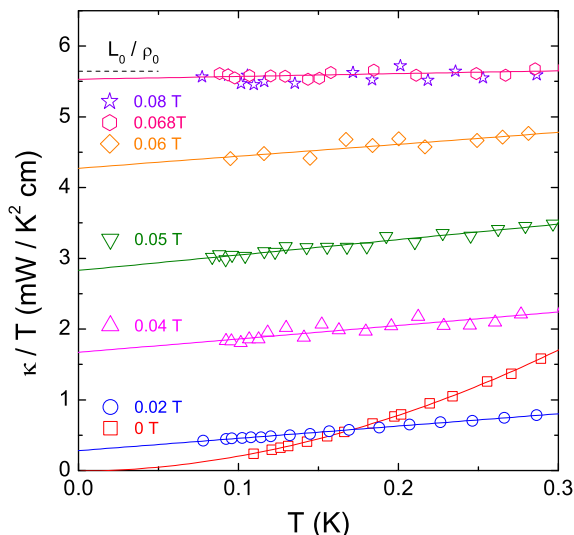


FIG. 3: (Color online). Low-temperature thermal conductivity of $\text{Ir}_{0.95}\text{Pt}_{0.05}\text{Te}_2$ single crystal in zero and magnetic fields. The solid lines are fits to $\kappa/T = a + bT^{\alpha-1}$. The dash line is the normal-state Wiedemann-Franz law expectation L_0/ρ_0 , with the Lorenz number $L_0 = 2.45 \times 10^{-8} \text{ W}\Omega\text{K}^{-2}$ and $\rho_0 = 4.34 \mu\Omega\text{cm}$.

resistivity with magnetic field parallel to the c axis up to $H = 0.75$ T and down to 50 mK, shown in Fig. 2(c). In zero field, the resistivity drops to zero at 2.94 K with a narrow transition width of 0.06 K. The superconducting transition is gradually suppressed in magnetic fields. In Fig. 2(d), we plot the temperature dependence of H_{c2} , where T_c is defined at the resistivity ρ dropping to zero on the curves in Fig. 2(c). The dashed line is a guide to the eye, which points to $H_{c2}(0) \approx 0.09$ T. This value is only about half of that in $\text{Ir}_{0.96}\text{Pt}_{0.04}\text{Te}_2$ polycrystal.⁸ It is not surprising since in polycrystal, due to the random grain orientation, the H_{c2} represents the maximum value for all field configurations, presumably $H \parallel ab$.

The thermal conductivities of $\text{Ir}_{0.95}\text{Pt}_{0.05}\text{Te}_2$ single crystal in zero and magnetic fields up to $H = 0.08$ T are plotted in Fig. 3, as κ/T versus T . We fit all the curves to $\kappa/T = a + bT^{\alpha-1}$, in which the two terms aT and bT^{α} represent contributions from electrons and phonons, respectively.^{19,20} The power α of the second term contributed by phonons is typically between 2 and 3 for single crystals, due to the specular reflections of phonons at the boundary.^{19,20} In zero field, the fitting gives a residual linear term $\kappa_0/T \equiv a = -7 \pm 18 \mu\text{W K}^{-2} \text{ cm}^{-1}$, with $\alpha = 2.91 \pm 0.04$. Since our experimental error bar is $5 \mu\text{W K}^{-2}\text{cm}^{-1}$, the κ_0/T in zero field is essentially zero, comparing to the normal-state Wiedemann-Franz law expectation $L_0/\rho_0 = 5.65 \text{ mW K}^{-2} \text{ cm}^{-1}$, with the Lorenz number $L_0 = 2.45 \times 10^{-8} \text{ W}\Omega\text{K}^{-2}$ and $\rho_0 = 4.34 \mu\Omega\text{cm}$.

For s -wave nodeless superconductors, there are no fermionic quasiparticles to conduct heat when $T \rightarrow 0$ since all electrons become Cooper pairs. Therefore,

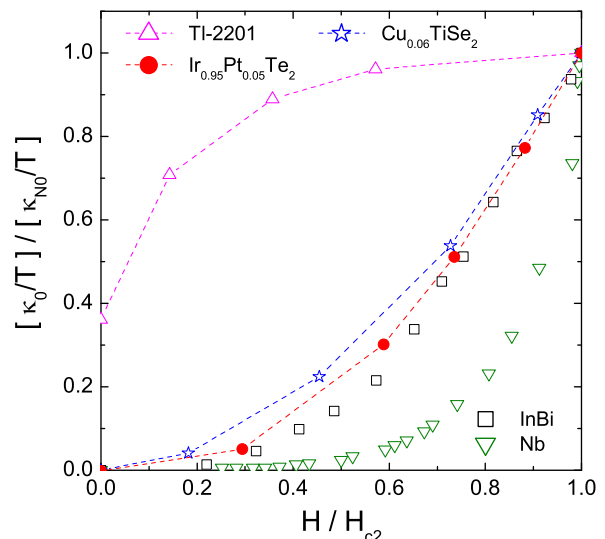


FIG. 4: (Color online). Normalized residual linear term κ_0/T of $\text{Ir}_{0.95}\text{Pt}_{0.05}\text{Te}_2$ as a function of H/H_{c2} . For comparison, similar data are shown for the clean s -wave superconductor Nb,²¹ the dirty s -wave superconducting alloy InBi,²² an overdoped d -wave cuprate superconductor Tl-2201,²³ and the single-gap s -wave superconductor $\text{Cu}_{0.06}\text{TiSe}_2$.¹⁷

there is no residual linear term of κ_0/T , as seen in Nb²¹ and InBi.²² However, a finite κ_0/T in zero field is usually observed in a superconductor with nodal gap, coming from the nodal quasiparticles.¹⁶ For example, $\kappa_0/T = 1.41 \text{ mW K}^{-2} \text{ cm}^{-1}$ for the overdoped cuprate $\text{Tl}_2\text{Ba}_2\text{CuO}_{6+\delta}$ (Tl-2201), a d -wave superconductor with $T_c = 15$ K,²³ and $\kappa_0/T = 17 \text{ mW K}^{-2} \text{ cm}^{-1}$ for the ruthenate Sr_2RuO_4 , a p -wave superconductor with $T_c = 1.5$ K.²⁴ The negligible κ_0/T of our $\text{Ir}_{0.95}\text{Pt}_{0.05}\text{Te}_2$ single crystal in zero field suggests a nodeless superconducting gap.

The field dependence of κ_0/T will give more information of the superconducting gap structure. For a clean type-II s -wave superconductor with isotropic gap, κ_0/T should grow exponentially with field (above H_{c1}), as in Nb.²¹ In the case of nodal superconductor, κ_0/T increases rapidly ($\sim H^{1/2}$) in low field due to the Volovik effect,²⁵ as in Tl-2201.²³

In Fig. 3, all the curves in magnetic field are roughly linear. Therefore we fit these curves to $\kappa/T = a + bT^{\alpha-1}$ with α fixed to 2. Previously $\alpha \approx 2.2$ was found in $\text{Cu}_{0.06}\text{TiSe}_2$,¹⁷ and recently $\alpha \approx 2$ has been observed in some iron-based superconductors such as $\text{BaFe}_{1.9}\text{Ni}_{0.1}\text{As}_2$,²⁶ KFe_2As_2 ,²⁷ and $\text{Ba}(\text{Fe}_{1-x}\text{Ru}_x)_2\text{As}_2$ single crystals.²⁸ Note that in the field of $H = 0.068$ T and 0.08 T, $\kappa_0/T = 5.53 \pm 0.03$ and $5.49 \pm 0.05 \text{ mW K}^{-2} \text{ cm}^{-1}$ were obtained, respectively. Both values are close to the normal-state Wiedemann-Franz law expectation $L_0/\rho_0 = 5.65 \text{ mW K}^{-2} \text{ cm}^{-1}$. We take $H = 0.068$ T as its bulk $H_{c2}(0)$. A slightly different $H_{c2}(0)$ does not affect our discussion on the field dependence of κ_0/T below.

In Fig. 4, the normalized κ_0/T of $\text{Ir}_{0.95}\text{Pt}_{0.05}\text{Te}_2$ single crystal is plotted as a function of H/H_{c2} . For comparison, we also plot the data of the clean s -wave superconductor Nb,²¹ the dirty s -wave superconducting alloy InBi,²² the d -wave cuprate superconductor Tl-2201,²³ and the s -wave superconductor $\text{Cu}_{0.06}\text{TiSe}_2$.¹⁷ From Fig. 4, the κ_0/T of $\text{Ir}_{0.95}\text{Pt}_{0.05}\text{Te}_2$ shows a field dependence similar to that of s -wave superconductors InBi and $\text{Cu}_{0.06}\text{TiSe}_2$. This further supports that $\text{Ir}_{0.95}\text{Pt}_{0.05}\text{Te}_2$ is a nodeless superconductor.

Nodeless gap does not essentially mean conventional superconductivity. For example, the nodeless gap observed in optimally doped iron-based superconductor may be unconventional s_{\pm} -wave resulting from antiferromagnetic spin fluctuations.²⁹ However, here in $\text{Ir}_{1-x}\text{Pt}_x\text{Te}_2$, the nodeless gap is unlikely s_{\pm} -wave. One obvious reason is that $\text{Ir}_{1-x}\text{Pt}_x\text{Te}_2$ does not have that kind of multiple Fermi surfaces as in iron-based superconductors.^{7,29} Therefore, the pairing symmetry in $\text{Ir}_{1-x}\text{Pt}_x\text{Te}_2$ is likely conventional s -wave. In this sense, the appearance of superconductivity may have little relationship with quantum fluctuations near QCP. This is not surprising since the single-gap s -wave superconductivity in Cu_xTiSe_2 is also not related to quantum fluctuations of CDW.

From the aspect of strong SOC, an unconventional odd-parity pairing state was claimed for the topological superconductor candidate $\text{Cu}_x\text{Bi}_2\text{Se}_3$.^{2,3} Both nodeless gap or gap with point nodes are allowed for the odd-parity superconducting state.² In this context,

more experiments such as point-contact spectra are needed to completely exclude novel superconductivity in $\text{Ir}_{1-x}\text{Pt}_x\text{Te}_2$.

IV. SUMMARY

In summary, we investigate the superconducting gap structure of $\text{Ir}_{1-x}\text{Pt}_x\text{Te}_2$ ($x = 0.05$) single crystal by thermal conductivity measurements. The κ_0/T in zero field is negligible, and the field dependence of κ_0/T is slow at low field. Both of them suggest nodeless superconductivity in $\text{Ir}_{1-x}\text{Pt}_x\text{Te}_2$. The pairing symmetry is likely conventional s -wave, although the odd-parity superconducting state can not be completely excluded from our measurements.

ACKNOWLEDGEMENTS

We thank J. J. Yang, Y. S. Oh, and S-W. Cheong for providing $\text{Ir}_{0.96}\text{Pt}_{0.04}\text{Te}_2$ polycrystal and nominal $\text{Ir}_{0.8}\text{Pt}_{0.2}\text{Te}_2$ single crystal to initialize this study. This work is supported by the Natural Science Foundation of China, the Ministry of Science and Technology of China (National Basic Research Program No: 2009CB929203 and 2012CB821402), and the Program for Professor of Special Appointment (Eastern Scholar) at Shanghai Institutions of Higher Learning.

* E-mail: shiyan_li@fudan.edu.cn

-
- ¹ Y. S. Hor, A. J. Williams, J. G. Checkelsky, P. Roushan, J. Seo, Q. Xu, H. W. Zandbergen, A. Yazdani, N. P. Ong, and R. J. Cava, *Phys. Rev. Lett.* **104**, 057001 (2010).
- ² S. Sasaki, M. Kriener, K. Segawa, K. Yada, Y. Tanaka, M. Sato, and Y. Ando, *Phys. Rev. Lett.* **107**, 217001 (2011).
- ³ M. Kriener, K. Segawa, S. Sasaki, and Y. Ando, *Phys. Rev. B* **86**, 180505(R) (2012).
- ⁴ P. Badica, T. Kondo, and K. Togano, *J. Phys. Soc. Jpn.* **74**, 1014 (2005).
- ⁵ H. Q. Yuan, D. F. Agterberg, N. Hayashi, P. Badica, D. Vandervelde, K. Togano, M. Sigrist, and M. B. Salamon, *Phys. Rev. Lett.* **97**, 017006 (2006).
- ⁶ M. Nishiyama, Y. Inada, and Guo-qing Zheng, *Phys. Rev. Lett.* **98**, 047002 (2007).
- ⁷ J. J. Yang, Y. J. Choi, Y. S. Oh, A. Hogan, Y. Horibe, K. Kim, B. I. Min, and S-W. Cheong, *Phys. Rev. Lett.* **108**, 116402 (2012).
- ⁸ S. Pyon, K. Kudo, and M. Nohara, *J. Phys. Soc. Jpn.* **81**, 053701 (2012).
- ⁹ M. Kamitani, M. S. Bahramy, R. Arita, S. Seki, T. Arima, Y. Tokura and S. Ishiwata, *Phys. Rev. B* **87**, 180501(R) (2013).
- ¹⁰ D. Ootsuki, Y. Wakisaka, S. Pyon, K. Kudo, M. Nohara, M. Arita, H. Anzai, H. Namatame, M. Taniguchi, N. L. Saini, and T. Mizokawa, *Phys. Rev. B* **86**, 014519 (2012).
- ¹¹ A. F. Fang, G. Xu, T. Dong, P. Zheng, and N. L. Wang, *Sci. Rep.* **2**, 1153 (2013).
- ¹² D. Ootsuki, S. Pyon, K. Kudo, M. Nohara, M. Horio, T. Yoshida, A. Fujimori, M. Arita, H. Anzai, H. Namatame, M. Taniguchi, N. L. Saini, and T. Mizokawa, arXiv:1207.2613.
- ¹³ Yoon Seok Oh, J. J. Yang, Y. Horibe, and S.-W. Cheong, *Phys. Rev. Lett.* **110**, 127209 (2013).
- ¹⁴ H. B. Cao, B. C. Chakoumakos, J. -Q. Yan, H. D. Zhou, R. Custelcean and D. Mandrus, arXiv:1302.5369.
- ¹⁵ P. Monthoux and G. G. Lonzarich, *Phys. Rev. B* **69**, 064517 (2004).
- ¹⁶ H. Shakeripour, C. Petrovic and L. Taillefer, *New J. Phys.* **11**, 055065 (2009).
- ¹⁷ S. Y. Li, G. Wu, X. H. Chen, and Louis Taillefer, *Phys. Rev. Lett.* **99**, 107001 (2007).
- ¹⁸ A. F. Kusmartseva, B. Sipos, H. Berger, L. Forró, and E. Tutiš, *Phys. Rev. Lett.* **103** 236401 (2009).
- ¹⁹ M. Sutherland, D. G. Hawthorn, R. W. Hill, F. Ronning, S. Wakimoto, H. Zhang, C. Proust, E. Boaknin, C. Lupien, L. Taillefer, R. X. Liang, D. A. Bonn, W. N. Hardy, R. Gagnon, N. E. Hussey, T. Kimura, M. Nohara, and H. Takagi, *Phys. Rev. B* **67**, 174520 (2003).
- ²⁰ S. Y. Li, J.-B. Bonnemaïson, A. Payeur, P. Fournier, C. H. Wang, X. H. Chen, and L. Taillefer, *Phys. Rev. B* **77**, 134501 (2008).
- ²¹ J. Lowell and J. Sousa, *J. Low. Temp. Phys.* **3**, 65 (1970).
- ²² J. Willis and D. Ginsberg, *Phys. Rev. B* **14**, 1916 (1976).
- ²³ C. Proust, E. Boaknin, R. W. Hill, L. Taillefer, and A. P.

- Mackenzie, Phys. Rev. Lett. **89**, 147003 (2002).
- ²⁴ M. Suzuki, M. A. Tanatar, N. Kikugawa, Z. Q. Mao, Y. Maeno, and T. Ishiguro, Phys. Rev. Lett. **88**, 227004 (2002).
- ²⁵ G. E. Volovik, JETP Lett. **58**, 469 (1993).
- ²⁶ L. Ding, J. K. Dong, S. Y. Zhou, T. Y. Guan, X. Qiu, C. Zhang, L. J. Li, X. Lin, G. H. Cao, Z. A. Xu and S. Y. Li, New J. Phys. **11**, 093018 (2009).
- ²⁷ J. K. Dong, S. Y. Zhou, T. Y. Guan, H. Zhang, Y. F. Dai, X. Qiu, X. F. Wang, Y. He, X. H. Chen, and S. Y. Li, Phys. Rev. Lett. **104**, 087005 (2010).
- ²⁸ X. Qiu, S. Y. Zhou, H. Zhang, B. Y. Pan, X. C. Hong, Y. F. Dai, M. J. Eom, J. S. Kim, Z. R. Ye, Y. Zhang, D. L. Feng, and S. Y. Li, Phys. Rev. X **2**, 011010 (2012).
- ²⁹ P. J. Hirschfeld, M. M. Korshunov, and I. I. Mazin, Rep. Prog. Phys. **74**, 124508 (2011).